UCRL-CONF-222309

LAWRENCE
LIVERMORE
NATIONAL
LABORATORY

Behavior of Explosives Under Pressure in a Diamond Anvil Cell

M.F. Foltz

June 2006

13th International Detonation Symposium, Norfolk, Virginia, 23-28 July 2006

DISCLAIMER

BEHAVIOR OF EXPLOSIVES UNDER PRESSURE
IN A DIAMOND ANVIL CELL

M. Frances Foltz[*]
[*]Lawrence Livermore National Laboratory, Livermore, CA 94551

Abstract. Diamond anvil cell (DAC) studies can yield information about the pressure dependence of materials and reactions under conditions comparable to shock loading. The pressure gradient across the face of the diamonds is often deliberately minimized to create uniform pressure over much of the sample and a simplified data set. To reach very high pressures (30-40 GPa), however, it may be necessary to use "softer", high nitrogen content diamonds that are more susceptible to bending under pressure. The resulting enhanced pressure gradient then provides a view of high-pressure behavior under anisotropic conditions similar to those found at the burn front in a bulk sample. We discuss visual observations of pressure-induced changes relative to variations in burn rate of several explosives (Triaminotrinitrobenzene, Nitromethane, CL-20) in the DAC. The burn rate behavior of both Nitromethane (NM) and Triaminotrinitrobenzene (TATB) were previously reported for pressures up to ~ 40 GPa. Nitromethane showed a near monotonic increase in burn rate to a maximum at ~30 GPa after which the burn rate decreased, all without color change. At higher pressures, the TATB samples had shiny (metallic) polycrystalline zones or inclusions where the pressure was highest in the sample. Around the shiny zones was a gradation of color (red to yellow) that appeared to follow the pressure gradient. The color changes are believed related to disturbances in the resonance structure of this explosive as the intermolecular separations decrease with pressure. The color and type of residue found in unvented gaskets after the burn was complete also varied with pressure. The four polymorphs of CL-20 (α, β, γ, ε-Hexanitrohexaazaisowurtzitane, HNIW) did not change color up to the highest pressure applied (~30 GPa), and each polymorph demonstrated a distinctly different burn rate signature. One polymorph (β) was so sensitive to laser ignition over a narrow pressure range that the sample could not be aligned with a low power laser without ignition. The burn rate for that one polymorph could only be measured at pressures above and below that unique pressure. This anomalous ignition threshold is discussed with respect to the matrix of possible polymorphs, most of which have not been isolated in the laboratory. The changes in behavior, color and reaction rates of all samples are discussed with respect to possible implications to chemistry at high pressure.

INTRODUCTION

After decades of study, the complex role that explosive chemistry plays in driving combustion and detonation reaction processes is still not fully understood. This lack of understanding hinders development of accurate predictive codes. To this end scientists continue to study the relationship between the detonation properties of high explosives (HE) under dynamic conditions to behavior observed under static high pressure. Observations across the entire detonation process need to be reconciled, from the start of initiation and evolution of reactions, to the

generation of reaction products behind the shock or combustion front. As part of this effort, diamond anvil cell (DAC) studies look at the pressure dependence of material properties and reactions.

Our previously published diamond anvil cell (DAC) work described burn rate as a function of pressure for several energetic molecules: nitromethane (NM),[1] Triaminotrinitrobenzene (TATB),[2] pentaerythritol-tetranitrate (PETN),[3] ammonium perchlorate (AP),[4] and hexanitrohexaazaisowurtzitane (HNIW, or CL–20).[5] Both the PETN and CL-20 studies included static-pressure mid-infrared FTIR spectra.

Here we relate additional qualitative information collected for TATB, Nitromethane, and CL-20 to provide calibration markers for current modeling efforts.

EXPERIMENTAL DETAILS

Details concerning the Bassett-type DAC and instrumentation used to measure pressure and burn rates have been described in earlier work.[1-5] Pressures up to ~40 GPa were applied to NM and TATB, and up to ~30 GPa to the four polymorphs of CL-20 (α, β, γ, ε).

For all materials studied but TATB, the

imaging Argon ion laser beam was transmitted through the sample. Due to the opacity of the TATB, the laser light was reflected from the ignition plane of the sample into the camera focusing optics. In addition, we took several still photos of TATB samples under pressure and of residue under pressure after removal from the DAC. These photos document interesting visual effects that were briefly mentioned in Reference 2. No other color changes were seen in any of the other energetic materials studied, including unpublished work on β-HMX (Octogen) and the liquid energetic explosive bis(2-fluoro-2,2-dinitroethyl) formal (FEFO).

In many high-pressure studies the pressure gradient across the sample is minimized to create a homogenous medium for accurately locating phase transitions. In order to do this, the sample diameter is small to minimize the effect of the pressure gradient. To reach high pressures (30-40 GPa), however, it may be necessary to use "softer", high-nitrogen content diamonds that are less susceptible to fracture with uneven loads. The pressure gradient of the non-hydrostatic environment caused by diamond deformation is more evident than with low-nitrogen diamonds. On the other hand, these samples offer a view of material behavior under anisotropic pressure conditions
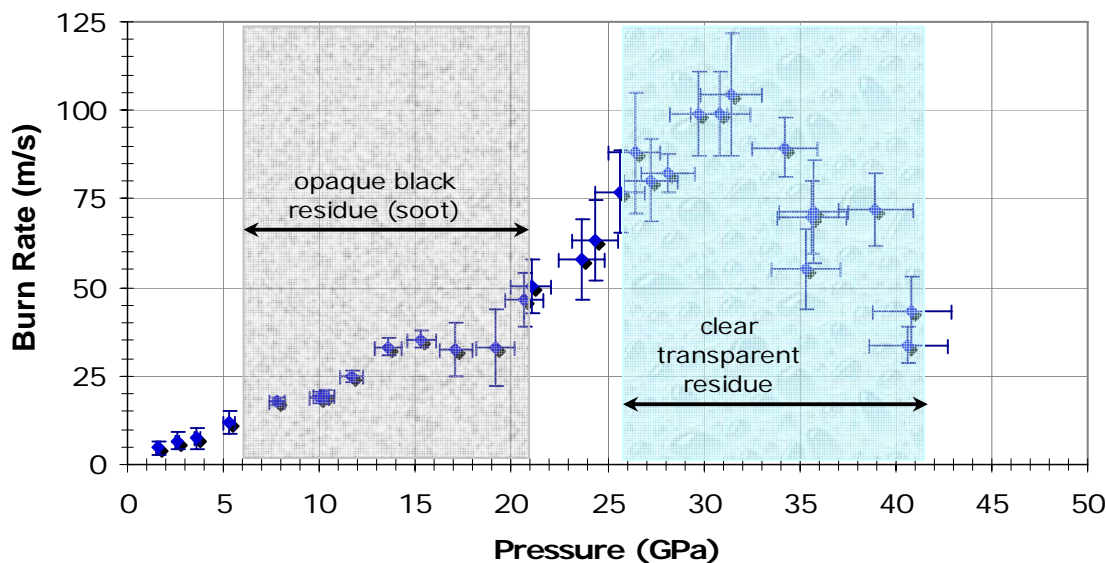

Figure 1. Nitromethane burn rate with concurrent change in the reaction products (Reference 1).

potentially found at the reaction front of an explosive. We used high-nitrogen diamonds in these experiments to reduce cost and time-consuming diamond alignments between test shots.

Figure 1 shows the nitromethane data from Reference 1. The plot is annotated to illustrate the different reaction residues found in the DAC gaskets.[1] As pressure was increased the residue changed. Below 2 GPa gaseous products vent the gasket and leave a white solid. In the pressure range of 5-19 GPa the residue is black (soot), with inaudible venting of gaseous products above 15 GPa. Above 19-20 GPa there is almost no soot when the gasket vents and a clear residue when it remains intact. Above 25 GPa the gasket no longer

vents gasses and the residue is clear and transparent, transforming to a white polycrystalline solid when pressure is released.

TATB

The burn rate for TATB was different from that of nitromethane in that it was slower and exhibited a distinct saw-tooth pattern with three burn rate maxima at ~18-, ~29- and ~39-GPa. [2] In the vicinity of each maximum was a transition region over which the color of the sample or products changed. These visual changes are superimposed on the published burn rate data in Figure 2, and briefly described in Table 1
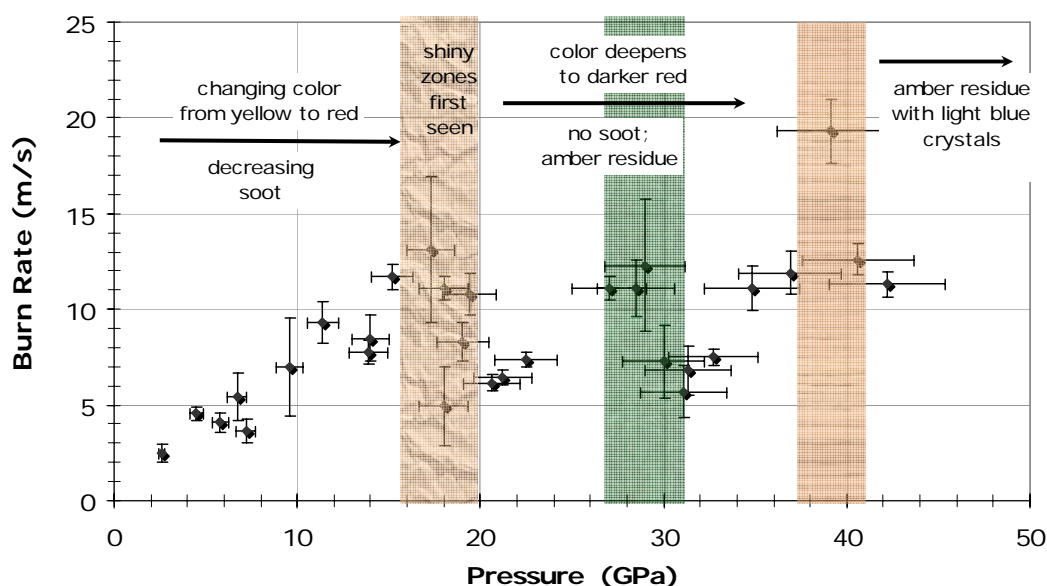

Figure 2. TATB burn rate shown with concurrent visual changes to the sample and residue.

With TATB the most notable observation was the appearance of shiny polycrystalline zones or inclusions in the central highest-pressure regions of the sample. These zones had a metallic, mirror-like finish. A color gradient of dark to lighter red extended radially from these shiny zones. This color gradient appeared to match the expected pressure gradient across the face of the diamonds. When pressure was released, the sample returned to the original yellow but the zone remained distinguishable from the bulk. An example of TATB pre-loaded to 16.4 GPa is shown in Figure 3. As pressure increased the shiny zones encompassed an increasing fraction of the sample area. These

zones exhibited a different compressibility with a ±7-10% pressure gradient compared to the typical ±5% seen for other materials in this DAC.

As the pressure was increased, reaction products did not always vent the gasket as was commonplace at lower pressures. Above ~30 GPa, the residue was a translucent amber solid in which the ruby chips (used for pressure measurements) were clearly visible. The gasket hole was also smaller diameter than before ignition. In one example, residue with an unidentified chip of blue material left for three days in the DAC had transformed from clear to polycrystalline.
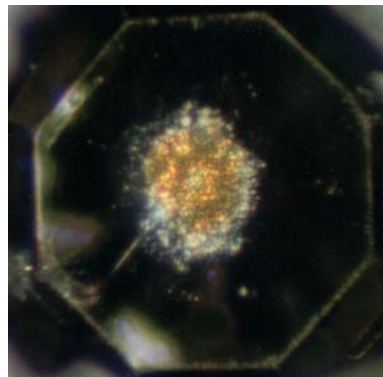
Figure 3. TATB pressurized to 16.4 GPa.

Table 1. Pressure-dependent change in TATB

Pressure (GPa)	Visual Observation	Burn Rate Behavior
~2.6 to 18	Increasingly colored, tinting from yellow to red.	Monotonically increasing burn rate and less soot residue.
~17 to 20	First see shiny (reflective) inclusions in high-pressure region.	Maximum then abrupt change to slower rate.
~18 to 28	Sample is red with shiny inclusions in the high-pressure region.	Monotonically increasing burn rate with no soot residue.
~27.6 to 31	No new color changes in the sample.	Maximum then abrupt change to slower burn rate. When gasket doesn't vent, an amber residue is left behind.
~30 to 37	Dark, opaque red zones surround the now highly reflective (mirror-like) inclusions in the high-pressure region.	Monotonically increasing rate.
~37 to 41	No new color changes in the sample.	Maximum then abrupt change to slower rate. When the gasket vents, no residue. When gasket doesn't vent, the residue is an amber polycrystalline material with light blue chips.

Figure 4. Amber and pale blue residue from TATB loaded to 31 GPa.

Shown in Figure 4 is an example of residue from TATB that had been pre-loaded to 31 GPa before ignition. We were unable to identify the solid residue by FTIR (Nicolet 60SX and IR PLAN microscope attachment) because the small sample size resulted in poor signal to noise.

CL-20

The relative thermal stability [6,7] and the burn rate as a function of pressure [5] of the four well-defined polymorphs of CL-20 (α, β, γ, ε) were previously published. We found that the epsilon (ε) polymorph to be the most thermodynamically stable phase, undergoing a phase transition to the gamma (γ) polymorph at 64 ± 1°C. [6]

Some of the large amount of data we collected is reproduced in Figure 5. The lines are guides to the eye meant to emphasize differences and commonalities of each polymorph. Note that in this pressure regime, alpha and gamma burn rates are almost indistinguishable (there is no separate line through the gamma data).

The four polymorphs exhibited similar burn rate profiles up to ~8 GPa. In particular the burn rate profiles of the alpha (α) and γ polymorphs were almost identical up to ~20 GPa. Over the range of 20-34 GPa the alpha sample followed the same pressure dependence as gamma but slower. The most dramatic "saw tooth" burn rate behavior took place at pressures >17 GPa with extreme swings from maxima to minima over small pressure increments (not shown). The fastest rates were ~1.2 km/s at 16-17 GPa for ε and γ samples. All samples remained colorless and transparent under pressure.

Under 2 GPa, reactions were incomplete with as much as ~75% of the starting material left in the

gasket. This residue consisted of soot-lined cracks in the sample propagating radially outward from the ignition zone. If gaseous products were made they did not make an audible snap when breaking through the gasket.

Above 2 GPa, all the CL-20 polymorphs burned increasingly to completion with decreasing soot residue. Above 6-8 GPa, not only did samples burn to completion but also product gases vented more forcefully with the rapidly increasing burn rate. There were no other notable changes to the reaction products up to the highest pressure attained ~40 GPa.

We also examined the infrared spectra (Nicolet 730 FTIR) of each polymorph under static pressure, monitoring two regions in particular to 13 GPa - the C-H stretch (3200-3000 cm^{-1}) and the ring + NO_2

deformation modes (700 - 830 cm^{-1}). We observed mostly monotonic changes in peak intensity, width, and frequency with increasing pressure interrupted with discontinuities. These and other anomalies appear to correspond to abrupt changes in burn rate.

We also discovered γ-CL-20 to be extra sensitive to light when pre-loaded ~8 GPa. The sample accidentally ignited about 50% of the time with either the defocused back-lighting Argon ion laser (514.5 nm, ~15 kW/cm^2) or the low power (<0.02 μJ) pulsed alignment laser. We could only measure the burn rate above and below this pressure, as the discontinuity illustrates in Figure 5. Burn rate data for β phase was similarly difficult to obtain > 8 GPa due to accidental ignition.
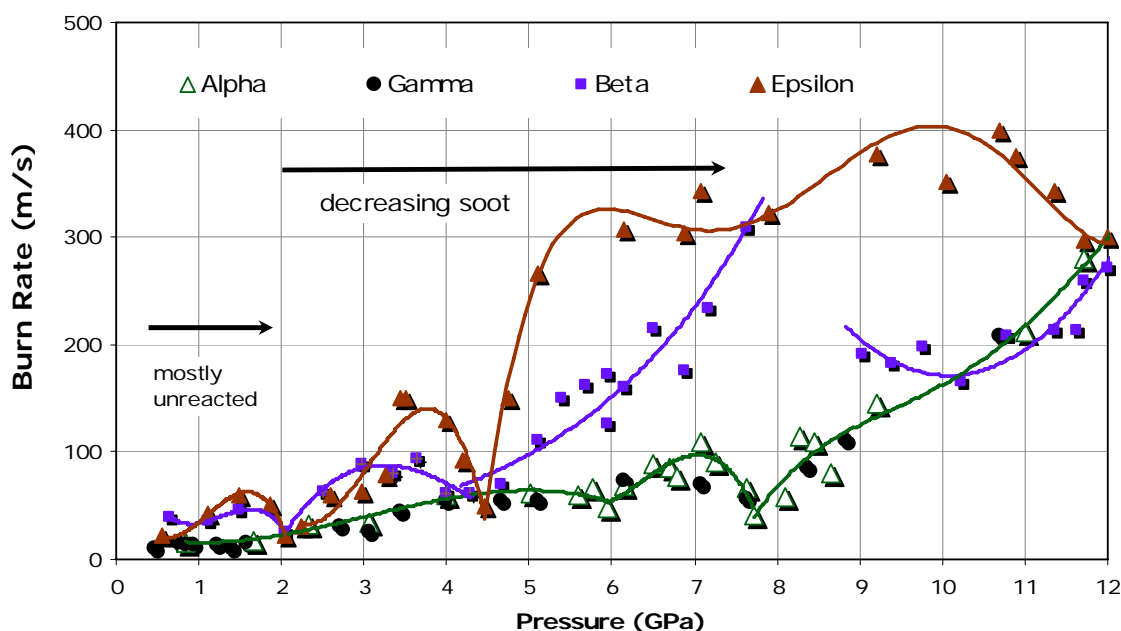

Figure 5. Pressure-dependent DAC burn rate of four CL-20 polymorphs.

DISCUSSION

These three energetic materials demonstrate easily differentiated burn rate behaviors in the diamond anvil cell, from pressure dependence to overall reaction rate from TATB (v_{max}~20 m/s at ~40 GPa) to CL-20 (v_{max}~1.2 km/s at ~17 GPa).

They also show common traits. The trend for all was a tendency to burn faster with pressure with interruptions correlating to changes in combustion

chemistry. Soot is preferentially produced at the lower pressures, with a cut-off at ~8 GPa for CL-20 and ~20 GPa for NM and TATB. At higher pressures all produced gaseous products, and eventually solid residue. For all materials, the transitions to different residue products correspond to abrupt changes in burn rate.

The behavior of intra- and intermolecular bonds under increasing pressure creates a roadmap to energetically favorable reaction pathways in

several ways. Under compression the crystal lattice distorts as the intermolecular distances decrease anisotropically. In response to further compression, molecules can twist and bend bonds to form a new polymorph (displacive transformation).[8] This change happens rapidly when the structure enters the new P,T field of stability. Or the relative alignment of molecules can involve bond breakage or reorganization molecules into a newly stable structure (reconstructive transformation). This causes molecules to rearrange into a new packing arrangement. These transformations can be sluggish with the old polymorph persisting unstably even in the P,T field of the new phase.

Nitromethane

Recent work by others has investigated the structural and vibrational properties of solid nitromethane under high pressure,[9] as well as the effect of uniaxial strain up to 200 GPa on the band gap.[10] Noteworthy in the latter work is that their static calculations show the C-H bond is highly stretched at a relatively early stage of uniaxial compression along the b lattice vector. They found that uniaxial compression did not cause a dramatic band-gap reduction associated with bending of the nitro group, and concluded that the onset for chemistry is strongly affected by pressure anisotropy.

With Raman spectroscopy, Courtecuisse et al.[11] have estimated the phase diagram of nitromethane over the pressure range of 0-35 GPa. This work includes three new low-temperature phases. According the phase diagram, a transition between chemical transformations between CII and transparent CI occurs at 11 GPa. Formation of the CI form from low-temperature phases is slow. Solid CI compound is recovered after releasing pressure at ambient pressure, but the Raman spectrum is indistinguishable from the ground state. While these observations appear consistent with this DAC work, the irreversible formation of CII, which is orange under white light transmission, does not appear to match. We saw no color changes under pressure. CII did not give any Raman signal and due to the small sample size could not be analyzed. It is not clear how these as-yet unidentified forms relate to the reaction chemistry of nitromethane under high pressure.

TATB

We discussed a number of different mechanisms in our previous paper to explain the change in color and appearance of shiny inclusions.[2] These included the possibility of phase transitions, formation of furoxan/furazan rings with exclusion of water, and realignment of the molecular rings with distortion of the crystal lattice under pressure and decrease intermolecular separation under compression.

Under ambient conditions TATB molecules pack into graphitic layers of a triclinic lattice, the in-plane aromatic rings aligned with those in every other plane.[12] The inter- and intra-molecular hydrogen bond system between amine and adjacent nitro groups within each plane yields a structure tolerant of mechanical insult. Hydrogen bonding between donor hydrogen and acceptor atoms is a well-defined phenomenon, and is the dominant force behind the insensitivity of TATB.[13] Other less well-defined π-π aromatic interactions play a key role in how molecules pack into a crystal lattice.

According to the semiconductor model of explosive initiation, the electrical conductivity of TATB is expected to sharply increase to values typical of semiconductors under conditions of shock wave compression.[14] The assumption is a combustion wave propagates from "hot-spot" microsites by means of electron heat conduction. For TATB, the energy gap is predicted to be $\varepsilon_g = 1.5$-2.0 eV in the pressure range of 10-20 GPa, which is close to the detonation threshold.[10] It is notable that the shiny inclusions may be a visual indicator of metallization, first appearing ~18 ± 2 GPa, in agreement with this theory.

Other studies have theoretically assessed the possible role of pressure-induced metallization in TATB. Wu et al.[15] compressed the crystal perpendicular to the TATB molecular sheet since it was believed to be the easiest direction to induce metallization. They found that band-gap closure begins near 47% uniaxial strain, with a lower pressure bound for metallization of ~120 GPa, far above the detonation pressure of TATB. A later study by Zhang et al.[16] of the crystalline structure of TATB concluded that the crystal exists as a semiconductor at 0.1-100 GPa with a predicted transition to conductor at hundreds of GPa. Neither study would appear to shed light on the visible changes seen in TATB under high pressure in the DAC.

While the semiconductor theory would predict onset for metallization where we first observe shiny inclusions in TATB in the DAC, it of course does not predict behavior at higher pressures above shock initiation. In order to explain behavior at higher pressure, we propose a collapse of the graphitic layers to one or more herringbone motifs commonly found among aromatic hydrocarbon molecules.

The packing patterns of geometrically similar planar aromatic hydrocarbons were studied by Gavezzotti et al.[17] They found that there are only a small number of well-defined ways these molecules pack into a crystal lattice: herringbone, sandwich-herringbone, sandwich-herringbone β, and sandwich-herringbone γ. These types differ mainly with respect to the relative orientation of molecular planes in the crystal, which is reflected in the length of the shortest cell axis. The simplest packing is the herringbone in which the molecules form stacks aligned edge-to-face with neighboring stacks. The sandwich herringbone is made up of pairs of parallel molecules. The γ packing is described as a sort of flattened herringbone. Lastly the β motif is a layered structure made up of graphitic planes. The TATB crystal structure falls into this category.

The interplanar distance is not infinitely compressible. If the first burn rate maximum at ~18 GPa is the alignment of aromatic rings in neighboring planes, maxima at 31- and 39-GPa could correspond to other polymorphic phase changes. One possibility includes the transition to different herringbone packings. In his study of planar aromatic compounds, Gavezzotti[17b] was able to group the different structures by the shortest lattice cell axis. The β herringbone (e.g. TATB) typically had the shortest axis, while the next shortest is the γ herringbone. To transition from graphitic to γ-herringbone would liberate previously H-bonded amine and nitro groups. Formation of highly oxygenated compounds like dinitrogen trioxide,[18] which is a blue solid, and furoxan/furazan rungs could become favorable reaction pathways.

Other small highly–colored molecules exist at high pressure but do not match the pressure regime of our observations. For example, at room temperature oxygen turns from a light-blue solid to orange at the β- to δ-O_2 transition (~5 GPa) then to red at the δ- to ε- O_2 transition (~10 GPa).[19] So the blue high-pressure inclusions we see in residue >17 GPa cannot be oxygen, however intriguing the idea. Nevertheless the deepening red of oxygen with increasing pressure, indicative of strong intermolecular interactions between O_2 molecules (O_4 clusters),[20] is similar to the deepening red of TATB. These parallel observations suggest that similar interactions between nitro groups may be taking place in herringbone-packed TATB molecules with an interrupted intermolecular H-bonding network.

CL-20

The burn rate behavior of CL-20 polymorphs indicates the orientation of nitramines about the rigid cage initially dominates chemical reaction pathways at the lower pressures applied. The basic structure of CL-20 is a rigid isowurtzitane cage with a nitro group attached to each of the six bridging nitrogens within the cage (Figure 6).[21] The nitramine appendages are flexible and the amine nitrogen can convert from a planar to a pyramidal conformation with little energy. The numbering on the cage nitrogens is used to identify the conformers. Each polymorph is distinguished by the endo-exo orientation of nitro groups about the six- and five-member rings of the cage and differences in crystal structure.[6] The four polymorphs display only three conformations, with the α form and γ form essentially identical but with different crystal packing and densities.
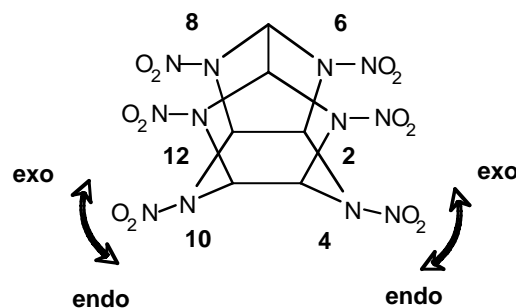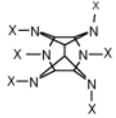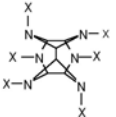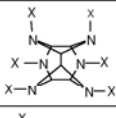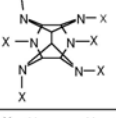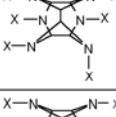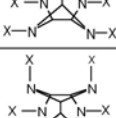

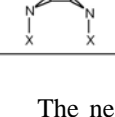**Figure 6. Numbering of CL-20 nitramine locations noted in Table 2.**

There are a number of possible polymorphs based on molecular conformation yet to be identified. Table 2 is simplified table of CL-20 conformers discussed in Reference 6, illustrating the exo-endo orientations of the NO_2 groups on the two 5-membered rings (left column) as a function of exo-endo orientations on the 6-membered ring.

Designators Y and N indicate the conformer is allowed by symmetry. A dash indicates a redundant structure. In addition to the four additional conformers predicted to be sterically stable (*) are five more we consider unlikely due to steric hindrance of the nitro groups.

Table 2. Top views of the conformers of CL-20 (Reference 6)

Structure	Polymorph (N-10) - (N-4) Orientation			
	exo-exo	exo-endo	endo-exo	endo-endo
	α * γ *	Y *	Y *	N
	β *	Y *	—	N
	Y *	ε *	—	N
	New 3 Y *	Y	Y *	N
	New 1 Y *	New 2 Y *	Y	N
	New 4 Y	Y	—	N
	Y *	Y	—	N

The near perfect match of pressure-dependent burn rate between identical α- and γ-conformers neatly illustrates that packing in the crystal lattice has little effect on reaction chemistry, especially since α-CL-20 usually exists as a hydrate. Using this analogy, the concurrent dips in burn rate of β- and ε-polymorphs at 2 GPa and 4.5 GPa suggests that the one nitramine orientation in common (N-8) is being affected by pressure, not the N-10 or N-4 groups on the 6-memberd ring. These transitions correspond to β → "New 1" and ε → "New 2" respectively. Thereafter the behaviors of these two polymorphs diverge as the β-phase passes through an anomalously light-sensitive transition region ~8 GPa. This behavior could indicate rotation of a nitro group causing more internal ring strain. One possible transition could be "New 1" → "New 3," the same 6-membered ring involved as the first transition. Another possibility is the "New 1" → "New 4" transition which forces the last nitro group into a highly symmetric but sterically hindered configuration.

CONCLUSIONS AND SUMMARY

When molecular reorientation, alignment or repacking occurs, formerly energetically favorable reaction pathways can become less favorable, resulting in different reaction rates and products. These changes can also affect sensitivity to external insults, whether mechanical (shock, impact), friction, or electronic (static, electromagnetic). Clearly the role of functional group interactions between neighboring molecules plays a role in determining initial reaction pathways.

This work provides more information to shed light onto high pressure reaction chemistry of energetic materials. We believe it shows that not realignment of molecules within the crystal lattice but also more subtle reorientation of functional groups can make significant changes to available reaction pathways under anisotropic pressure conditions similar to that found at the reaction front of explosives.

REFERENCES

1. Rice, S.R., Foltz, M.F., "Very High Pressure Combustion: Reaction Propagation Rates of Nitromethane within a Diamond Anvil Cell" *Combustion and Flame*, Vol. 87, pp. 109-122, 1991.

2. Foltz, M.F., "Pressure Dependence of the Reaction Rate of TATB at High Pressure," *Propellants, Explosives, Pyrotechnics,* Vol. 18, pp. 210-216, 1993.

3. Foltz, M.F., "Pressure Dependence on the Reaction Propagation Rate of PETN at High Pressure," *Proceedings of the 10th Detonation Symposium*, pp. 579-585, Boston, MA, July 1993.

4. Foltz, M.F., Maienschein, J.L., "Ammonium Perchlorate Phase Transitions to 26 GPa and 700 K in a Diamond Anvil Cell," *Materials Letters*, Vol. 24, pp. 407-414 (1995).

5. Foltz, M.F., "High Pressure Combustion of CL-20 Polymorphs in a Diamond Anvil Cell," *1991 JANNAF CL-20 Symposium*, China Lake, CA, May 1991.

6. Foltz, M.F., Coon, C.L., Garcia, F., Nichols III, A.L., "The Thermal Stability of the Polymorphs of Hexanitrohexaazaisowurtzitane, Part I," *Propellants, Explosives, Pyrotechnics,* Vol. 19, pp. 19-25 (1994).

7. Foltz, M.F., Goon, C.L., Garcia, F., Nichols III, A.L., "The Thermal Stability of the Polymorphs of Hexanitrohexaazaisowurtzitane, Part II," *Propellants, Explosives, Pyrotechnics,* Vol. 19, pp. 133-144 (1994).

8. Bloss, F.D., "Structural Variations, Composition, and Stability," in *Crystallography and Crystal Symmetry*, pp. 318-320, Holt, Rinehart and Winston, New York, 1971.

9. Liu, H., Zhao, J., Wei, D., Gong, Z., "Structural and vibrational properties of solid nitromethane under high pressure by density functional theory," *Journal of Chemical Physics*, 124(12), 124501, 2006.

10. Margetis, D., Kaxiras, E., Elstner, M., Frauenheim, Th., Manaa, M.R., "Electronic structure of solid nitromethane: Effects of high pressure and molecular vacancies," *Journal of Chemical Physics,* 117(2), pp. 788-799, 2002.

11. Courtecuisse, S., Cansell, F., Fabre, D., Petitet, J.-P., "Phase transitions and chemical transformations of nitromethane up to 350 °C and 35 GPa," *Journal of Chemical Physics,* 102(2), pp. 968-974, 1995.

12. Cady, H.H., Larson, A.C., "The Crystal Structure of 1,3,5-Triamino-2,4,6-trinitrobenzene," *Acta Crystallographica,* 18, pp. 485-496, 1965.

13. Kolb, J.R., Rizzo, H.F., "Growth of 1,3,5-Triamino-2,4,6-trinitrobenzene (TATB) I. Anisotropic Thermal Expansion," *Propellants and Explosives*, 4, pp. 10-16, 1979.

14. Grebenkin, K.F., Zherebstov, A.L., Kutepov, A.L., Popova, V.V., "On the Experimental Verification of the Semiconductor Model of Detonation," *Technical Physics,* 47(11), 1458-1460, 2002.

15. Wu, C.J., Yang, L.H., Fried, L.E., Quenneville, J., Martinez, T.J., "Electronic structure of solid 1,3,5-triamino-2,4,6-trinitrobenzene under uniaxial compression: Possible role of pressure-induced metallization in energetic materials," *Physical Review B*, 67, pp. 235101, 2003.

16. Zhang, C., Shu, Y., Zhao, X., Wang, X., "Theoretical Study on Crystalline Structures of TATB at Different Pressures," *Science and Technology of Energetic Materials*, 66(2), pp. 261-265, 2005

17.a. Desiraju, G.R., Gavezzotti, A., "From Molecular to Crystal Structure; Polynuclear Aromatic Hydrocarbons," *Journal of the Chemical Society - Chemical Communications*, 10, pp. 621-623, 1989; b. Desiraju, G.R., Gavezzotti, A., "Crystal Structures of Polynuclear Aromatic Hydrocarbons. Classification, Rationalization and Prediction from Molecular Structure," *Acta Crystallographica*, B45, pp. 473-482, 1989.

18. Wang, X., Qin, Q.-Z., "A new conformer of dinitrogen trioxide in low temperature matrix: trans-cis N_2O_3," *Spectrochimica Acta Part A,* 54, pp. 575-580, 1998.

19. Desgreniers, S., Vohra, Y.K., Ruoff, A.L., "Optical Response of Very High Density Solid Oxygen to 132 GPa," *Journal of Physical Chemistry*, 94, pp. 1117-1122, 1990.

20. Santoro, M., Gregoryanz, E., Mao, H.-k., Hemley, R.J., *"*New Phase Diagram of Oxygen at High Pressures and Temperatures*,"* *Physical Review Letters*, 93, pp. 265701, 2004.

21. Gilardi, R., "Polytypical Polymorphs Occurring in an Energetic Material," *Virtual Course on Polymorphism: Diversity Amidst Similarity*, International School of Crystallography, Erice, Italy, June 2004